JACS
JOURNAL OF THE AMERICAN CHEMICAL SOCIETY
Article
pubs.acs.org/JACS

Hydrogen Evolution from Aliphatic Alcohols and 1,4-Selective Hydrogenation of NAD$^+$ Catalyzed by a [C,N] and a [C,C] Cyclometalated Organoiridium Complex at Room Temperature in Water

Yuta Maenaka,[†] Tomoyoshi Suenobu,[†] and Shunichi Fukuzumi*[,†,‡]

[†]Department of Material and Life Science, Graduate School of Engineering, Osaka University, ALCA, Japan Science and Technology Agency (JST), Suita, Osaka 565-0871, Japan

[‡]Department of Bioinspired Science, Ewha Womans University, Seoul 120-750, Korea

Supporting Information

ABSTRACT: A [C,N] cyclometalated Ir complex, [Ir^{III}(Cp*)(4-(1*H*-pyrazol-1-yl-κN^2)benzoic acid-κC^3)(H$_2$O)]$_2$SO$_4$ [**1**]$_2$·SO$_4$, was reduced by aliphatic alcohols to produce the corresponding hydride complex [Ir^{III}(Cp*)(4-(1*H*-pyrazol-1-yl-κN^2)-benzoate-κC^3)H]$^-$ **4** at room temperature in a basic aqueous solution (pH 13.6). Formation of the hydride complex **4** was confirmed by ^{1}H and ^{13}C NMR, ESI MS, and UV−vis spectra. The [C,N] cyclometalated Ir-hydride complex **4** reacts with proton to generate a stoichiometric amount of hydrogen when the pH was decreased to pH 0.8 by the addition of diluted sulfuric acid. Photoirradiation (λ > 330 nm) of an aqueous solution of the [C,N] cyclometalated Ir-hydride complex **4** resulted in the quantitative conversion to a unique [C,C] cyclometalated Ir-hydride complex **5** with no byproduct. The complex **5** catalyzed hydrogen evolution from ethanol in a basic aqueous solution (pH 11.9) under ambient conditions. The 1,4-selective catalytic hydrogenation of β-nicotinamide adenine dinucleotide (NAD$^+$) by ethanol was also made possible by the complex **1** to produce 1,4-dihydro-β-nicotinamide adenine dinucleotide (1,4-NADH) at room temperature. The overall catalytic mechanism of hydrogenation of NAD$^+$, accompanied by the oxidation of ethanol, was revealed on the basis of the kinetic analysis and detection of the reaction intermediates.

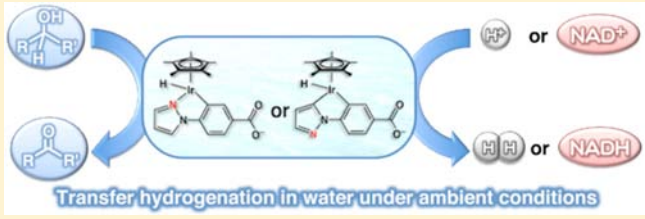

INTRODUCTION

Hydrogen has merited increasing attention as a clean, inexhaustible, efficient, and cost-attractive energy carrier for the future.[1] Green and sustainable ways of producing hydrogen have so far been extensively explored through the development of catalytic,[2] photocatalytic,[3−7] and electrocatalytic reaction systems.[8] The majority of commercially produced hydrogen is generated from fossil fuel (e.g., natural gas, liquid hydrocarbons, and coal) by steam reforming, which requires high temperatures (700−1200 K), generating CO and CO_2 as waste products.[9] Hydrogen can also be produced from naturally available alcohols, so-called bioethanol, as an alternative to fossil feedstocks, which are carbon-neutral materials, because these alcohols are produced by the CO_2-consuming photosynthesis. Extensive efforts have so far been devoted to developing catalysts for hydrogen production from alcohols (eq 1 for ethanol).[10−15]

$$CH_3CH_2OH \rightarrow H_2 + CH_3CHO \quad (1)$$

However, hydrogen production from alcohols is largely endergonic (68.6 kJ mol^{-1} at 298 K in gas phase)[16] so that the thermodynamics demands elevated temperatures.[17] Thus, there has so far been no report on hydrogen production from alcohols at ambient temperature in water.[18−20] Recently, an efficient hydrogen evolution system from ethanol has been achieved by using an oxyhydride heterogeneous catalyst ($CeNiH_ZO_Y$) at 333 K.[21] However, pretreatment of the catalyst under H_2 is necessary at 523 K for a long period of time (10 h). The mechanism of the catalytic formation of hydrogen from alcohols in water has yet to be clarified. On the other hand, bioethanol is usually produced by fermentation in water with the aid of enzymes and, thus, contains a certain amount of water, at least 5 vol%.[22,23] The mixture of water and ethanol is a well-known azeotrope, and the use of the mixture as a biofuel to produce hydrogen is practically preferred to that of pristine ethanol to avoid costly isolation procedures.

We recently reported a hydrogenase functional mimic, a water-soluble iridium aqua complex [Ir^{III}(Cp*)(4-(1*H*-pyrazol-1-yl-κN^2)benzoic acid-κC^3)(H$_2$O)]$_2$SO$_4$ [**1**]$_2$·SO$_4$, which can catalyze both the reduction of protons with 1,4-dihydro-β-nicotinamide adenine dinucleotide (NADH) to produce H_2 and the regioselective reduction of β-nicotinamide adenine dinucleotide (NAD$^+$) to produce NADH by H_2 under atmospheric pressure at room temperature depending on pH (eq 2).[24] The catalytic interconversion between formic acid and H_2 was also achieved using **1** as a catalyst (eq 3).[25] The complex **1** was doubly deprotonated from both the carboxyl group and the aqua ligand

Received: March 22, 2012
Published: May 13, 2012

   dx.doi.org/10.1021/ja302788c | J. Am. Chem. Soc. 2012, 134, 9417−9427

as pH increased from 2.0 to 12 to afford **2** and **3**, respectively (Chart 1).[24,25] The Ir-hydride complex **4** was shown to be the reactive intermediate in both catalytic systems.

Chart 1

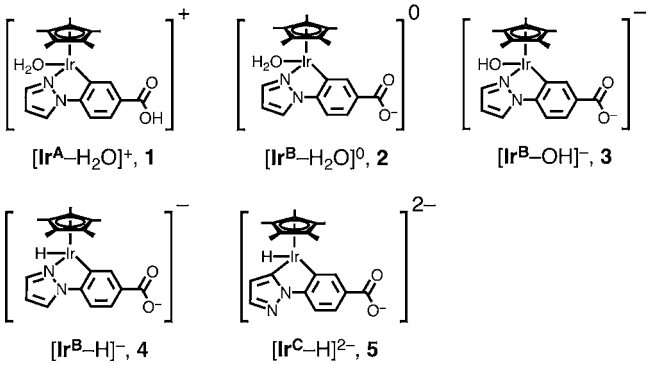

$$NADH + H^+ \rightleftarrows NAD^+ + H_2 \quad (2)$$

$$HCOOH \rightleftarrows H_2 + CO_2 \quad (3)$$

In the natural photosynthetic system, regeneration of a coenzyme NAD(P)H from NAD(P)$^+$ is preferred to H_2 generation to store chemically the energy of electrons and protons taken from water using solar energy except for photosynthetic organisms containing hydrogenase by which both the oxidation of H_2 with NAD(P)$^+$ and the reduction of protons to form H_2 with NAD(P)H are catalyzed.[26] The regeneration of coenzyme NADH from NAD$^+$ has so far been achieved by nonenzymatic chemical[27−31] and photochemical[32−35] methods in contrast to alcohol dehydrogenase (ADH), which catalyzes the conversion of ethanol, a weak hydride donor, to acetaldehyde coupled with the 1,4-regioselective reduction of NAD$^+$ to NADH (eq 4).

$$NAD^+ + C_2H_5OH \rightarrow NADH + CH_3CHO + H^+ \quad (4)$$

Extensive efforts have so far been devoted to develop functional mimics of ADH that are able to reduce NAD$^+$ analogues to NADH analogues with alcohols as a reductant in organic solvents.[36−39] However, there has so far been no report on ADH functional mimics that can catalyze the hydrogenation of NAD$^+$ to produce 1,4-NADH selectively by ethanol at room temperature in water.

We report herein for the first time the catalytic hydrogen evolution from aliphatic alcohols with a [C,C] cyclometalated iridium hydride complex **5** (Chart 1), which is produced by photoconversion of the [C,N] cyclometalated iridium hydride complex **4**. The complex **1** has been found to catalyze the regioselective reduction of NAD$^+$ by ethanol to generate 1,4-NADH in water at room temperature as the first functional mimic of alcohol dehydrogenase (ADH).

EXPERIMENTAL SECTION

Materials. The following reagents were obtained with the best available purity and used without further purification unless otherwise noted: hydrogen hexachloroiridate, H_2IrCl_6 (4N grade, Furuya Metal Co., Ltd.), 1,2,3,4,5-pentamethylcyclopentadiene (>90%, Kanto Chemical Co., Inc.), 4-(1*H*-pyrazol-1-yl)benzoic acid (90% Aldrich Chemicals Co.), 3-(trimethylsilyl)propionic-2,2′,3,3′-d_4 acid sodium salt (TSP, > 98%, Aldrich Chemicals Co.), β-nicotinamide adenine dinucleotide disodium salt hydrate, reduced form (Tokyo Chemical Industry Co., Ltd.), β-nicotinamide adenine dinucleotide, oxidized form (Oriental Yeast Co., Ltd.), boronic acid, potassium chloride, sodium hydroxide, sodium chloride, sulfuric acid, 2-propanol, 2-butanol, ethanol, methanol, 1-propanol, 1-butanol, 2-methly-2-propanol (Wako Pure Chemical Industries), sodium hydroxide-*d* in D_2O (40 wt % NaOD, 99.5% D; Aldrich Chemical Co.), D_2O (99.9% D; Cambridge Isotope Laboratories), methanol-d_4 (99% D; Cambridge Isotope Laboratories), ethanol-d_6 (99.8% D; Cambridge Isotope Laboratories), methanol-1,1,1-d_3 (99.8% D; TAIYO NIPPON SANSO Cooperation).

General Methods. All experiments were performed under an Ar atmosphere by using standard Schlenk techniques unless otherwise noted. Purification of water (18.2 MΩ cm) was performed with a Milli-Q system (Millipore; Direct-Q 3 UV). ^1H and ^{13}C NMR spectra were recorded on a JEOL JNM-AL300 spectrometer and a Varian UNITY INOVA600 spectrometer, respectively. UV−vis absorption spectra were recorded on a Hewlett-Packard 8453 diode array spectrophotometer with a quartz cuvette (light-path length =1 cm) at 298 K. Electrospray ionization mass spectrometry (ESI-MS) data were obtained using an API 150EX quadrupole mass spectrometer (PE-Sciex), equipped with an ion spray interface. The sprayer was held at a potential of +5.0 or −4.4 kV for positive or negative ion detection modes, respectively, and compressed N_2 was employed to assist liquid nebulization. The orifice potential was maintained at +30.0 or −40.0 V for positive or negative modes, respectively. Nanosecond laser flash photolysis experiments were performed using a Panther OPO pumped by Nd:YAG laser (Continuum, SLII-10, 4−6 ns fwhm) at λ = 355 nm with the power of 10 mJ per pulse. The transient absorption measurements were performed using a continuous wave xenon lamp (150 W) and a photomultiplier (Hamamatsu 2949) as a probe light and a detector, respectively. The output from a photomultiplier was recorded on a digitizing oscilloscope (Tektronix, TDS3032, 300 MHz). Femtosecond transient absorption spectroscopy experiments were conducted using an ultrafast source, Integra-C (Quantronix Corp.); an optical parametric amplifier, TOPAS (Light Conversion Ltd.); and a commercially available optical detection system, Helios provided by Ultrafast Systems LLC. The source for the pump and probe pulses were derived from the fundamental output of Integra-C (λ = 786 nm, 2 mJ/pulse and fwhm = 130 fs) at a repetition rate of 1 kHz. Seventy-five percent of the fundamental output of the laser was introduced into a second harmonic generation (SHG) unit, Apollo (Ultrafast Systems), for excitation light generation at λ = 393 nm, while the rest of the output was used for white light generation. The laser pulse was focused on a sapphire plate of 3 mm thickness, and then white light continuum covering the visible region from λ = 410 to 800 nm was generated via self-phase modulation. A variable neutral density filter, an optical aperture, and a pair of polarizer were inserted in the path in order to generate stable white light continuum. Prior to generating the probe continuum, the laser pulse was fed to a delay line that provides an experimental time window of 3.2 ns with a maximum step resolution of 7 fs. In our experiments, a wavelength at λ = 393 nm of SHG output was irradiated at the sample cell with a spot size of 1 mm diameter where it was merged with the white probe pulse in a close angle (<10°). The probe beam after passing through the 2 mm sample cell was focused on a fiber optic cable that was connected to a CMOS spectrograph for recording the time-resolved spectra (λ = 410−800 nm). Typically, 1500 excitation pulses were averaged for 3 s to obtain the transient spectrum at a set delay time. Kinetic traces at appropriate wavelengths were assembled from the time-resolved spectral data.

pH Adjustment. The pH values were determined by a pH meter (TOA, HM-20J) equipped with a pH combination electrode (TOA, GST-5725C). The pH of the solution was adjusted by using 1.00 M H_2SO_4/H_2O and 1.00−10.0 M NaOH/H_2O without buffer unless otherwise noted. The pD of the solution was adjusted by using 95−97 wt % D_2SO_4 and 40 wt % NaOD without buffer unless otherwise noted. Values of pD were corrected by adding 0.4 to the observed values (pD = pH meter reading +0.4).[40]

Synthesis. [Ir^{III}(Cp*)(4-(1*H*-pyrazol-1-yl-κN^2)benzoic acid-κC^3)-(H_2O)]$_2SO_4$ [**1**]$_2$·SO_4 was synthesized according to the literature.[25]

Synthesis of Ir-Hydride Complex 4 by Reaction of 3 with Ethanol. Ethanol (10 μL) was added to D_2O (0.55 mL) containing **3** (9.2 mM) at pD 13.6, and the solution was kept for 5 h. pD was adjusted

by adding NaOD aqueous solution. After reaction, ^{1}H NMR spectrum was recorded, and the yield was determined to be 98% by integrating the signals of Cp* of **3** and **4**. ^{1}H NMR of **4** (600 MHz, in D_2O, reference to TSP in D_2O at pD 13.6, 298 K): (ppm) −14.34 (s, 1H), 1.91 (s, η^5-$C_5(CH_3)_5$, 15H), 6.64 (dd, J = 2.4 Hz, J = 2.4 Hz, 1H), 7.41 (d, J = 8.4 Hz, 1H), 7.57 (dd, J = 8.4 Hz, J = 1.8 Hz, 1H), 7.76 (d, J = 2.4 Hz, 1H), 8.21 (d, J = 1.8 Hz, 1H), 8.25 (d, J = 2.4 Hz, 1H). ^{13}C NMR of **4** (600 MHz, in D_2O, reference to TSP in D_2O at pD 13.6, 298 K): (ppm) 11.67 (s, η^5-$\underline{C}_5(CH_3)_5$), 92.86 (η^5-$C_5(\underline{C}H_3)_5$), 111.00, 113.10, 125.99, 129.03, 135.79, 140.37, 142.01, 143.76, 147.53, 178.95. ESI-MS in methanol containing NaOH (1.5 μM): m/z 515 $[\mathbf{4}]^-$ (Figure S2 in Supporting Information).

Synthesis of [C,C] Cyclometalated Ir-Hydride Complex 5 by Photoirradiation of 4. A D_2O solution containing **4** (9.2 mM) at pD 13.6 was irradiated with a Xe lamp (Ushio Optical, Model X SX-UID 500X AMQ) through a colored glass filter (Toshiba Glass UV-35) transmitting λ > 340 nm at room temperature for 7 h. After the photochemical reaction, the ^{1}H NMR spectrum of the resulting solution was recorded, and the yield of the [C,C] cyclometalated Ir-hydride complex **5** was determined to be 98% by integrating the signals of Cp* of **4** and **5**. ^{1}H NMR of **5** (300 MHz, in D_2O, reference to TSP in D_2O at pD 13.6, 298 K): (ppm) −17.48 (s, 1H), 2.01 (s, η^5-$C_5(CH_3)_5$, 15H), 6.14 (d, J = 1.6 Hz, 1H), 7.24 (d, J = 8.0 Hz, 1H), 7.50 (dd, J = 8.0 Hz, J = 1.8 Hz, 1H), 7.58 (d, J = 1.6 Hz, 1H), 8.21 (d, J = 1.8 Hz, 1H). ^{13}C NMR of **5** (600 MHz, in D_2O, reference to TSP in D_2O at pD 13.6, 298 K): (ppm) 12.10 (s, η^5-$\underline{C}_5(CH_3)_5$), 93.46 (d, J_{C-H} = 3.8 Hz η^5-$C_5(\underline{C}H_3)_5$), 111.15, 112.57, 125.23, 132.20, 138.674, 140.663, 144.64, 155.00, 156.91, 179.95. The signal at 93.46 is a doublet indicating that the carbon nuclear spin is coupled with a proton nuclear spin of H atom directly bonded to iridium as previously reported.[41] ESI-MS [Ir(Cp*)(4-(1*H*-pyrazol-1-yl-κC^5)benzoate-κC^3)(CO)]$^-$ **7** in 2-propanol containing NaOH (1.5 μM): m/z 541 $[\mathbf{7}]^-$ (Figure S7 in Supporting Information). **7** was prepared by flowing CO at atmospheric pressure for 1 h to the solution of **5**. Since the complex **5** as well as **4** is very sensitive to contaminated oxygen and gradually reacts with proton to evolve hydrogen, there might not be enough time for isolation, purification, and crystallization of **4** or **5** in water to obtain crystals with an enough size appropriate for X-ray crystal structure analysis.

Formation of Ir-Hydride Complex 4 in the Reaction of 1 with Alcohols. Typically, ethanol (0.10 mL) was added to 1.0 M NaOH solutions (2.0 mL) containing **1** (120 μM) at 298 K. The concentrations of the hydride complex **4** were determined from the absorbance at λ = 350 nm ($\varepsilon = 4.7 \times 10^3$ M^{-1} cm^{-1}). For measurements of the dependence of formation rate of **4** on concentration of ethanol, the concentration of ethanol was changed from 0.41 mM to 1.2 M. For measurements of the dependence of formation rate of **4** on concentration of **3**, the concentration of **3** was changed from 29 μM to 1.4 mM. The formation rate of **4** was determined at various temperatures from 278 to 308 K.

Formation of Aldehyde and Ketones in the Oxidation of Aliphatic Alcohols by 3. Typically, 2-propanol (10 μL) was added to a 1.0 M NaOH aqueous solution (0.6 mL) containing **3** (2.6 mM), and the solution was kept for 10 min. 2-Butanol (10 μL) was added to a 1.0 M NaOH aqueous solution (0.6 mL) containing **3** (2.3 mM) at 298 K, and the solution was kept for 30 min. The yield of products was determined by ^{1}H NMR measurements of the product solution with TSP as an internal standard using a sealed capillary tube (i.d. = 1.5 mm) filled with D_2O for deuterium lock. ^{1}H NMR spectra were recorded at room temperature. Molar ratios of the hydroxo complex **3** and the hydride complex **4** were determined by integrating the signals of Cp* of **3** and **4**.

Quantum Yield Determination. A standard actinometer (potassium ferrioxalate) was used for the quantum yield determination of photoconversion from **4** to **5**. A square quartz cuvette (path length = 1.0 cm) that contained a deaerated aqueous solution of **2** (0.11 mM) containing 2-propanol (0.62 M) at pH 13.5 was irradiated with monochromatized light of λ = 330 nm using a Shimadzu RF-5300PC fluorescence spectrophotometer. The light intensity of monochromated light of λ = 330 nm was determined as 1.2×10^{-8} einstein s^{-1} with a slit width of 20 nm. The photochemical reaction was monitored by an increase in absorbance at λ = 300 nm. To avoid the contribution of light absorption of the products, only the initial rates were used for the determination of the quantum yield, where the absorbance of **4** at λ = 330 nm has been taken into account.

Hydrogen Evolution from Alcohols by Changing pH. Typically, 2-propanol (0.10 mL) was added to 0.1 M NaOH solutions (2.0 mL) containing **1** (0.26 mM) at 298 K, and the mixture was stirred for 15 min. Then, pH was adjusted to be 0.8 by addition of H_2SO_4 (10 M) aqueous solution, and the gas in the headspace was analyzed using a Shimadzu GC-14B gas chromatograph (N_2 carrier, active carbon with a particle size of 60−80 mesh at 353 K) equipped with a thermal conductivity detector. No CO gas was detected by Shimadzu GC-17A gas chromatograph {Ar carrier, a column with molecular sieves (Agilent Technologies, 19095P-MS0) at 313 K} equipped with a thermal conductivity detector.

Catalytic Hydrogen Evolution from Alcohols under Basic Conditions. Typically, 2-propanol or ethanol (0.50 mL) was added to an aqueous solution containing **3** (55 μM) at pH 11.9 and stirred for 15 min. Then, aqueous solutions were irradiated with a Xe lamp (Ushio Optical, ModuleX SX-UID 501X AMQ) through a colored glass filter (Toshiba Glass UV-35) transmitting λ > 340 nm at room temperature for 30 min to convert **4** to **5**. After photoirradiation, aqueous solutions were vigorously stirred at various temperatures, and the gas in the headspace was analyzed using a Shimadzu GC-14B gas chromatograph. Without photoirradiation, no hydrogen evolution was observed at 323 K as shown in Figure 7 (red line).

Hydrogenation of NAD$^+$ in Basic Water Catalyzed by 2 and 3 in the Presence of Ethanol. Typically, ethanol (0.50 mL) was added to 0.5 M borate buffer solutions (1.5 mL) containing **2** (15 μM) and NAD^+ (77 μM) at 298 K at pH 10.0. The amounts of NADH were determined from the absorbance at λ = 340 nm ($\varepsilon = 6.23 \times 10^3$ M^{-1} cm^{-1}). Turnover frequency (TOF) values were determined by measuring the amounts of NADH for the initial 5 min. For measurements of the dependence of formation rate on concentration of ethanol, the concentration of ethanol was changed from 0.44 to 5.7 M. For measurements of the formation rate on concentration of [**2**] + [**3**], the concentration of the sum of [**2**] and [**3**] was changed from 7.5 to 30 μM. For measurements of the dependence of formation rate on concentration of NAD^+, the concentration of NAD^+ was changed from 39 μM to 4.5 mM. For measurements of pH dependence of the formation rate, pH was changed from 8.5 to 10.0.

RESULTS AND DISCUSSION

Formation of Ir-Hydride Complex 4. As pH was increased, the aqua complex $[\mathbf{Ir^A}\text{-}OH_2]^+$ **1** released protons from the carboxyl group and the aqua ligand to form the corresponding benzoate complex $[\mathbf{Ir^B}\text{-}OH_2]^0$ **2** and the hydroxo complex $[\mathbf{Ir^B}\text{-}OH]^-$ **3**, respectively (Scheme 1). The pK_a values of

Scheme 1. Acid-Base Equilibria of Iridium Aqua Complexes

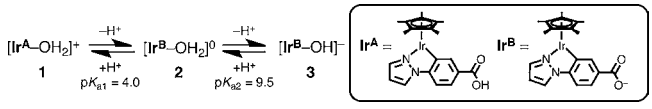

complexes **1** and **2** were determined from the spectral titration to be pK_{a1} = 4.0 and pK_{a2} = 9.5, respectively.[24] When ethanol was added to an aqueous solution of **3** at pD 13.6, **3** was reduced to produce the corresponding Ir-hydride complex $[\mathbf{Ir^B}\text{-}H]^-$ **4** as shown by the ^{1}H NMR spectral change (Figure 1a) at high yield (98%). The ^{1}H NMR spectrum of the Ir-hydride complex **4** agrees with that obtained in the reaction of **3** with atmospheric pressure of H_2 at pD 13.6.[25] It should be noted that further hydration and condensation of the product acetaldehyde has precluded the observation and characterization of the product by GC−MS and ^{1}H NMR under basic conditions.[42−44]

dx.doi.org/10.1021/ja302788c | J. Am. Chem. Soc. 2012, 134, 9417−9427

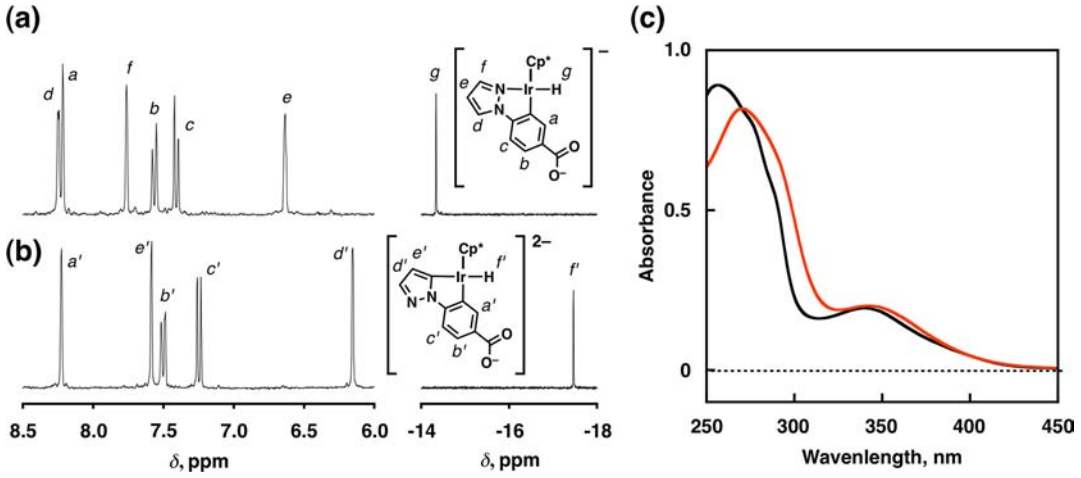

Figure 1. (a) ^{1}H NMR spectra of **4**, which was produced in the reaction of **3** (9.2 mM) with ethanol (0.31 M) for 5 h in D_2O at 298 K and pD 13.6. (b) ^{1}H NMR spectra of **5**, which was produced from **4** (9.2 mM) by photoirradiation (λ > 340 nm) for 7 h at pD 13.6. (c) UV−vis spectra of diluted aqueous solutions containing **4** (black line, 45 μM) and **5** (red line, 45 μM), which were detected by ^{1}H NMR as shown in panels a and b, respectively, at 298 K and pH 13.7.

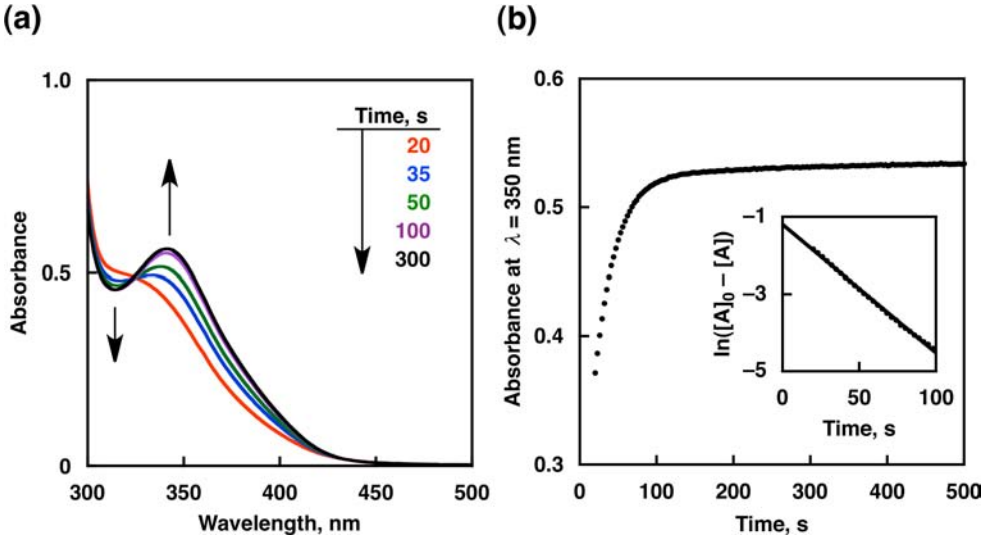

Figure 2. (a) UV−vis spectral changes in the reaction of **3** (0.12 mM) with ethanol (0.82 M) in a diluted aqueous solution containing NaOH at 298 K (pH 13.7). (b) Time profile of absorbance at λ = 350 nm during the reaction of **3** (0.12 mM) with ethanol (0.82 M) in a diluted aqueous solution containing NaOH at 298 K (pH 13.7). Inset shows the first-order plot.

After the reaction of **3** with ethanol, the diluted aqueous reaction solution containing the Ir-hydride complex **4** (pH 13.7) exhibits a characteristic UV−vis absorption band at λ_{max} = 340 nm as shown in Figure 1c (black line). Similarly, other alcohols (2-propanol and 2-butanol) also react with **3** in water at pH 14.0 to afford the nearly stoichiometric amount of corresponding ketones (acetone and 2-butanone) and **4** at high yields (84% and 96%, respectively; see Experimental Section and Figure S1 in Supporting Information). Thus, the stoichiometry of the Ir-hydride complex formation from alcohols is given by eq 5.

$$\mathbf{3} + C_2H_5OH \rightarrow \mathbf{4} + CH_3CHO + H_2O \quad (5)$$

The reaction of **3** with CH_3OH and CD_3OD also afforded the Ir-H and Ir-D complexes as indicated by the ESI mass spectrum, respectively (Figure S2 in Supporting Information).

The reaction of **3** in the presence of a large excess of ethanol was followed by the UV−vis spectral change due to formation of the Ir-hydride complex **4** (λ_{max} = 340 nm) as shown in Figure 2. The rate of absorption change at λ = 340 nm obeyed first-order kinetics, and the first-order rate constants (k_{obs}) in the presence of various concentrations of ethanol were determined from the first-order plots (Figure S3 in Supporting Information). The dependence of k_{obs} on concentration of ethanol (EtOH) is shown in Figure 3, where the k_{obs} value is proportional to [EtOH]. From the slope of this plot, the second-order rate constants (k_H) of formation of the hydride complex **4** were determined in the reaction of **3** with aliphatic alcohols in an aqueous solution (pH 13.7) at 298 K as shown in Table 1 and Figure S4 (Supporting Information). The k_H value increases with increasing temperature. The activation parameters for the reaction of **3** with ethanol were determined to be $\Delta H^{\ddagger}$ = 82 kJ mol^{-1} and $\Delta S^{\ddagger}$ = 1.5 J K^{-1} mol^{-1} from the Eyring plot (Figure 4).[45] When CH_3OH was replaced by CD_3OH in the reaction of **3** at pH 13.7, a kinetic deuterium isotope effect (KIE) for k_H was observed to be 3.2 (= k_H/k_D) as shown in Figure S5 (Supporting Information). When C_2H_5OH was replaced by CD_3CD_2OH in the reaction of **3** at pH 13.7, a kinetic deuterium isotope effect (KIE) for k_H was observed to be 2.1 (= k_H/k_D) as shown in Figure S6 (Supporting

dx.doi.org/10.1021/ja302788c | J. Am. Chem. Soc. 2012, 134, 9417−9427

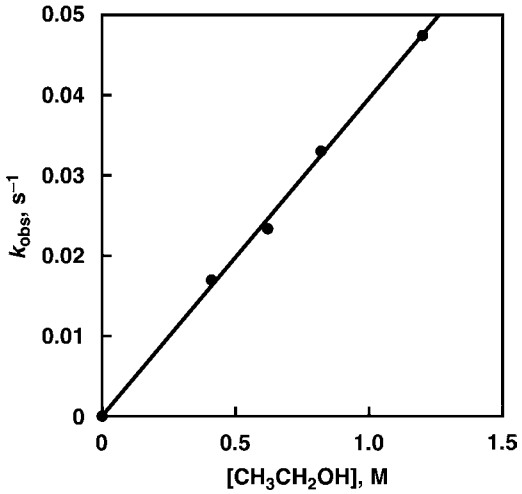

Figure 3. Plot of the observed rate constant (k_{obs}) in the reaction of **3** (0.12 mM) with ethanol in a diluted aqueous solution containing NaOH at 298 K (pH 13.7) versus concentration of ethanol.

Table 1. Rate Constant (k) of Formation of the Hydride Complex with Aliphatic Alcohols at 298 K

entry	alcohol	k, M^{-1} s^{-1}
1[a]	CH_3OH	6.5×10^{-3}
2[a]	CD_3OH	2.0×10^{-3}
3[b]	CH_3OD	6.1×10^{-3}
4[a]	CH_3CH_2OH	3.9×10^{-2}
5[b]	CH_3CH_2OD	3.3×10^{-2}
6[c]	CD_3CD_2OH	1.9×10^{-2}
7[a]	$CH_3CH_2CH_2OH$	4.8×10^{-2}
8[a]	$CH_3CH(CH_3)OH$	2.4×10^{-2}
9[a]	$CH_3(CH_2)_3OH$	5.2×10^{-2}
10[a]	$(CH_3)_3COH$	no reaction

[a]pH 13.7. [b]pD 13.9 (in D_2O, 98%). [c]pH 13.7 (in H_2O, 98%).

Information). The observation of KIEs indicates that the reaction of **3** with methanol and ethanol involves the C−H bond cleavage. Thus, the β-hydrogen elimination of the methoxy and ethoxy complexes, which are produced by the replacement of a hydroxy (OH) ligand of **3** by a methoxy (CH_3O) and ethoxy (CH_3CH_2O) ligand, respectively, may be the rate-determining step for formation of **4** (Scheme 2).

Scheme 2

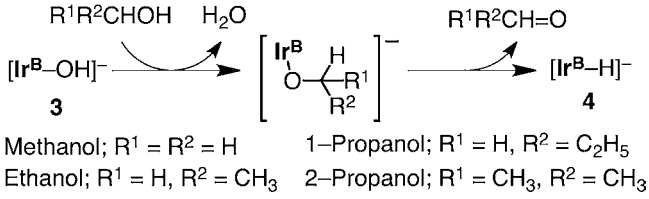

Photoconversion from the [C,N] to the [C,C] Cyclometalated Organoiridium Hydride Complex. When an aqueous solution of **4** produced by the reaction of ethanol with **3** in D_2O at pD 13.6 was photoirradiated for 7 h with a Xe lamp through a colored glass filter transmitting $\lambda > 340$ nm, the signal of the C5 proton (δ = 8.25 ppm, see Chart 1) disappeared completely and the signal of hydride proton exhibited upfield shift as shown in Figure 1b. Thus, the hydride complex **4** was converted to the [C,C] cyclometalated complex **5** (Scheme 3) in

Scheme 3

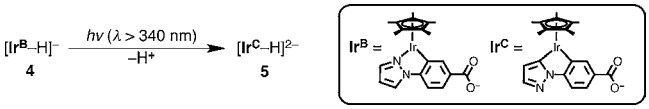

98% yield. A diluted aqueous solution containing the hydride complex **5** (pH 13.7) shows a UV−vis spectrum with the absorption band at λ_{max} = 350 nm as shown in Figure 1c (red line). Photoirradiation with a monochromatized light at λ = 350 nm to an aqueous solution of **4** leads to an increase in the absorption band at λ = 305 nm and a decrease in the absorption band at λ_{max} = 255 nm with an isosbestic point at λ = 268 nm as shown in Figure 5. The final UV−vis spectrum agrees with the spectrum of the [C,C] cyclometalated complex **5** (Figure 1c).

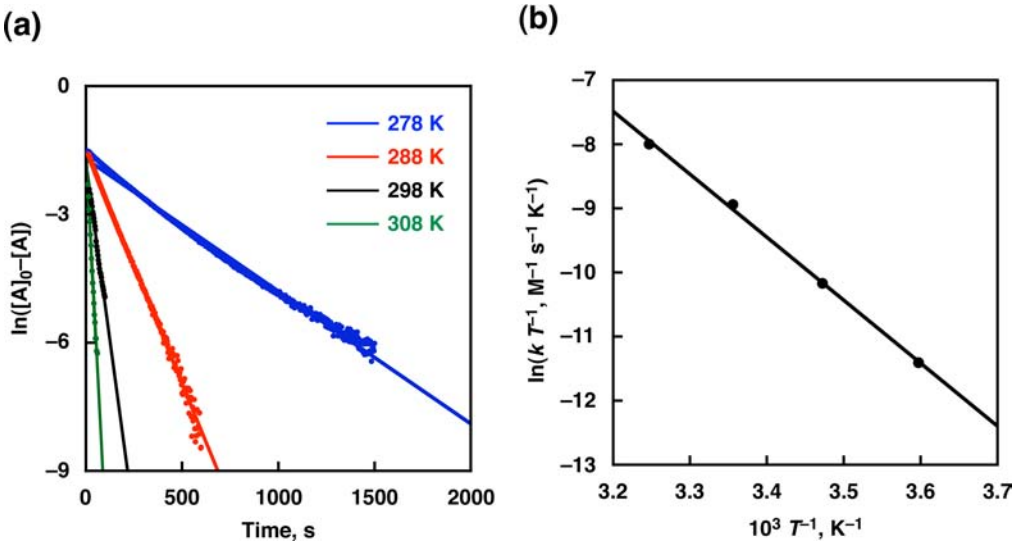

Figure 4. (a) First-order plots in the reaction of **3** with ethanol (0.82 M) in a diluted aqueous solution containing NaOH (pH 13.7) at 278 K (blue line), 288 K (red line), 298 K (black line), and 318 K (green line). (b) Eyring plot for the formation of the Ir-hydride complex in the reaction of **3** with ethanol.

dx.doi.org/10.1021/ja302788c | J. Am. Chem. Soc. 2012, 134, 9417−9427

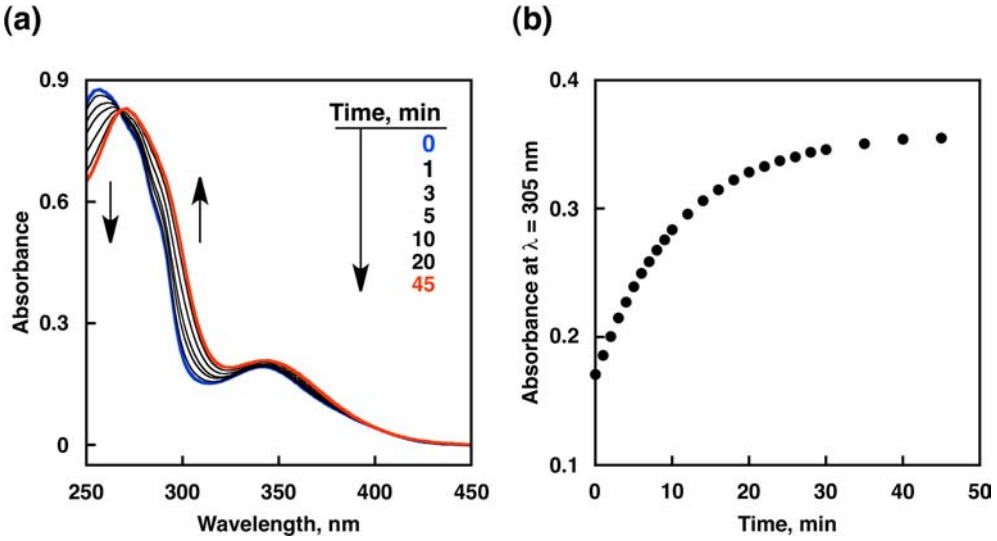

Figure 5. (a) UV−vis spectral changes of **4** to **5** under photoirradiation (λ = 350 nm) of a diluted aqueous solution containing **4** (38 μM), NaOH (1.0 M), and ethanol (0.82 M) at 298 K and pH 13.7. (b) Time profile of absorbance at λ = 305 nm during the conversion from **4** to **5** under photoirradiation (λ = 350 nm) of a diluted aqueous solution containing **4** (0.12 mM), NaOH (1.0 M), and ethanol (0.82 M) at 298 K and pH 13.7.

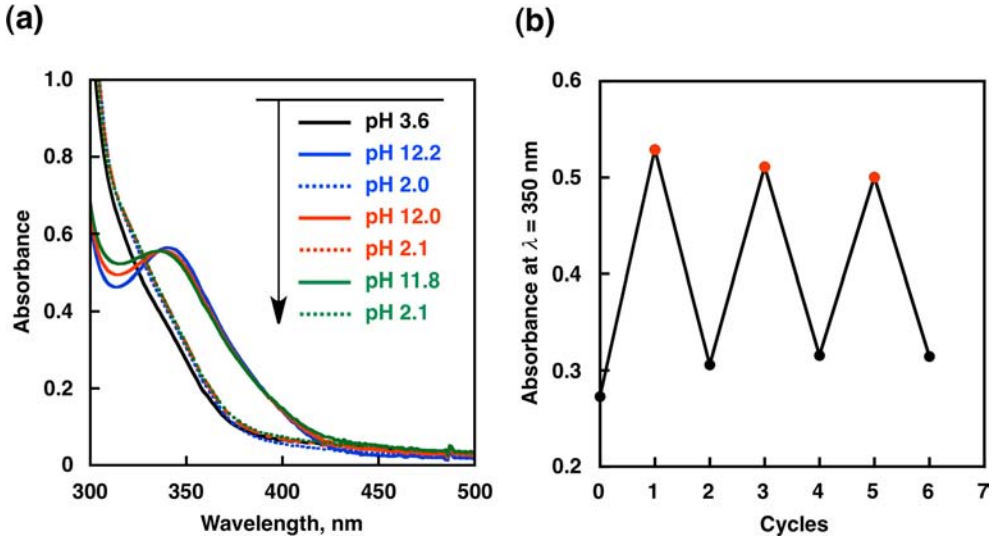

Figure 6. (a) UV−vis absorption spectral changes of an aqueous solution of **3** (0.12 mM) and ethanol (0.82 M) by alternate change in pH. (b) Change in absorbance at λ = 350 nm due to formation of the hydride complex **4** (red closed circle) in the reaction of **3** (0.12 mM) with ethanol (0.82 M) in water (pH 11.8−12.2) and that due to the hydrogen evolution (black closed circle) in the reaction of the hydride complex **4** with proton in water at 298 K (pH 2.0−3.3) by adding an aqueous solution of H_2SO_4 (5.0 M) or NaOH (5.0 M).

The ESI mass spectrum of the CO bubbled aqueous solution of **5** agrees with the calculated isotopic distribution for the corresponding CO complex, i.e., [Ir(Cp*)(4-(1*H*-pyrazol-1-yl-κC^5)benzoate-κC^3)(CO)]$^-$ (Figure S7 in Supporting Information).

The quantum yield of this photoreaction, i.e., the photoconversion of the [C,N] cyclometalated complex **4** to the [C,C] cyclometalated complex **5** in deaerated H_2O, was determined to be 1.7% by using a standard actinometer (see Experimental Section). Nanosecond laser excitation at λ = 355 nm of a deaerated aqueous solution containing **4** and ethanol resulted in rapid formation of a new absorption band at λ_{max} = 340 nm as shown in Figure S8 (Supporting Information). No decay was observed for 1.0 ms after laser excitation at 1.6 μs, indicating that the photoconversion from **4** to **5** has been completed within 1.6 μs after laser excitation. Actually, the transient absorption spectrum at 1.6 μs (λ = 340−500 nm) is in good agreement with the differential spectrum obtained by subtracting the absorption spectrum of **4** from that of **5** as shown in Figure 1c. Thus, femtosecond laser flash photolysis was performed in a deaerated aqueous solution of **4** to observe the phenomena in shorter time scale. A broad absorption band at λ = 580 nm appeared at 0.33 ps upon irradiation with a laser pulse (λ_{ex} = 388 nm). The rapid spectral decay of the absorption band (λ = 580 nm) synchronized with the recovery of the bleaching due to the ground state absorption by **4** at λ_{max} = 480 nm with an isosbestic point at ca. λ = 540 nm from 0.33 to 1.5 ps can be assigned to the intersystem crossing (ISC) from the singlet excited state of **4** (λ_{max} = 580 nm) to the triplet excited state (Figure S9a in Supporting Information). The time profile at λ = 560 nm was fitted by a single exponential decay (Figure S9b in Supporting Information) to afford the ISC rate constant, k_{ISC} = 2.0 × 10^{12} s^{-1}.

dx.doi.org/10.1021/ja302788c | J. Am. Chem. Soc. 2012, 134, 9417−9427

The relatively fast ISC rate can be rationalized by the contribution of a strong spin−orbit coupling of iridium metal ion in the excited state of **4**.[46,47] The observed spectra at 1.5 ps to 3.0 ns are almost unchanged as shown in Figure S9c (Supporting Information), indicating that the conversion from **4** to **5** may occur at prolonged reaction time for 3.0 ns to 1.6 μs, which is beyond the measurable time scale (<3.0 ns) of the femtosecond laser flash photolysis.

Hydrogen Evolution from Aliphatic Alcohols. The hydride complex **4** is stable at pH 14; however, when pH was decreased to 0.8 by adding H_2SO_4, the hydride complex **4** was converted to an aqua complex **1** as shown by Figure 6a accompanied by evolution of hydrogen (H_2). The yield of H_2 was determined by GC to be 82% yield. It was also confirmed by GC that no CO (<1000 ppm) was produced during the reaction. The conversion between the hydride complex **4** and the aqua complex **1** accompanied by H_2 evolution was repeated by alternate change in pH between ca. 12 and ca. 2 in the presence of excess amount of ethanol as shown in Figure 6. The conversion from **1** to **4** in the reaction of ethanol with **1** and that from **4** to **1** accompanied by H_2 evolution by changing pH is shown in Scheme 4. Under

Scheme 4

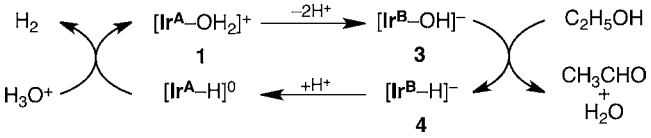

basic conditions (pH 14), the aqua complex **1** exists as the hydroxo complex **3** (pK_{a2} = 9.5) that possesses the benzoate and hydroxo ligands, which reacts with ethanol to produce acetaldehyde and the hydride complex **4**. Under acidic conditions (pH 1.0), the hydride complex reacts with proton to produce H_2, accompanied by regeneration of **1**.

In contrast to the [C,N] cyclometalated Ir-hydride complex **4**, the [C,C] cyclometalated Ir-hydride complex **5** can react with water to produce H_2 under basic conditions as shown in Figure 7. The turnover number (TON) of H_2 evolution with **5** increases linearly with time to reach 3.3 (2.5 h), whereas **4** has no catalytic reactivity even at elevated temperature at 323 K. TON for hydrogen evolution with **5** increases with increasing temperature to be 26 (1.0 h) at 353 K. This catalytic reactivity of **5** may be attributed to the electron-donating effect of the phenylpyrazole ligand on the metal center in **5** with the [C,C] cyclometalated iridium as indicated by the upfield shift (shielding effect) of the hydride signal bonded to Ir^{III} center (vide supra), even though the hydrogen atom bonded to Ir shows larger upfield shift due to the relativistic effect.[48]

Catalytic Hydrogenation of NAD^+. Recently, we reported that the hydride complex **4**, which was produced by the reaction with atmospheric pressure of hydrogen, can reduce NAD^+ to produce the 1,4-isomer of NADH at room temperature.[24] Thus, we expected to use ethanol as a hydride donor to generate NADH. When we added an aqueous solution containing **2** and **3** to the borate buffer (0.5 M, pH 10) and ethanol mixed solution [3: 1 (v/v)], formation of **4** was confirmed by the UV−vis spectrum (blue line in Figure 8a, λ_{max} = 340 nm). Addition of the NAD^+ solution to the mixed solution resulted in formation of NADH as shown in Figure 8b, accompanied by an increase in the absorption band at λ = 340 nm due to NADH (red and green lines in Figure 8a). NAD^+ was converted to NADH at 86% yield in the first cycle

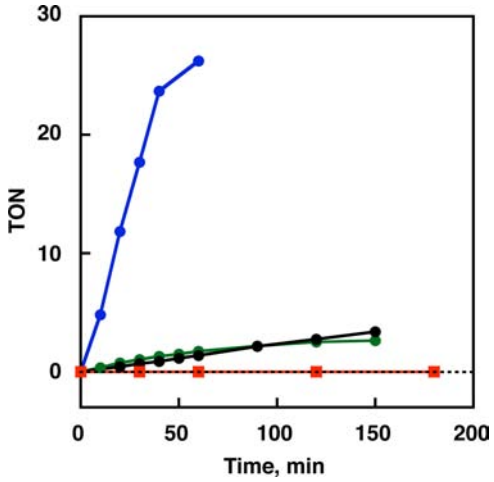

Figure 7. Time course of hydrogen evolution from 2-propanol (4.3 M) catalyzed by **5** (55 μM) in water (pH 11.9) at 353 K (blue line) and 323 K (black line) and that from ethanol (5.7 M) catalyzed by **5** (55 μM) in water (pH 11.9) at 323 K (green line). The complex **5** was formed from **4** under photoirradiation (λ > 340 nm) for 30 min. Time course of hydrogen evolution from 2-propanol (4.3 M) catalyzed by **4** (55 μM) in water (pH 11.9) at 323 K is shown by the red line.

and at 79% in the second cycle. From the linear slope for initial 5 min after addition of NAD^+, the TOF value was determined to be 18 h^{-1}. The progress of the reaction was monitored by the rise in the absorbance at λ = 340 nm due to NADH as shown by the time course of absorbance at λ = 340 nm in Figure S10 (Supporting Information). The rate of formation of NADH increased linearly with increasing concentration of **2** and **3** at pH 10.0 as shown in Figure 9a. In the absence of complex **2** or **3**, no formation of NADH was observed. The rate of formation of NADH also linearly increased with increasing concentration of ethanol (Figure 9b). These linear relationships indicate that the rate-determining step in the catalytic hydrogenation of NAD^+ with ethanol is formation of the Ir-H complex **4**, which reacts with NAD^+ rapidly to produce NADH, accompanied by regeneration of **2** and **3** (Scheme 5). Thus, the amount of **4** in a steady state in the catalytic cycle is negligible. The observed first-order rate constant (k_{obs}) of formation of the Ir-H complex **4** in the presence of ethanol (5.7 M) at pH 10.0 at 298 K was determined from the first-order plot in Figure S11 (Supporting Information) to be 21 h^{-1}. This confirms that the rate-determining step in the catalytic cycle is the formation of **4**. The TOF value decreased with decreasing pH to 8.5 as shown by the slope of the linear plots in Figure 10a. The increase in the rate with further increase in pH from 8.5 results from the deprotonation of the aqua complex (Ir-OH_2, pK_a = 9.5) to afford the hydroxo complex (Ir-OH) **3**, which may be active for the oxidation of ethanol (Figure 10b). The pH range for the catalytic hydrogenation of NAD^+ with ethanol in Figure 10b is limited because of the acid-catalyzed hydration of NADH under acidic conditions[49] and decomposition of NAD^+ under alkaline conditions.[50] The standard Gibbs energy change ($\Delta G'^{\circ}$) for the reaction (eq 4) at pH 7 at 298 K was determined to be +25 kJ mol^{-1} from the reported equilibrium constant.[51] Because the $\Delta G'^{\circ}$ value at pH 10 is still positive (+8 kJ mol^{-1}), a large excess of ethanol is required to complete the hydrogenation of NAD^+ with ethanol under the conditions in Figure 10.

dx.doi.org/10.1021/ja302788c | J. Am. Chem. Soc. 2012, 134, 9417−9427

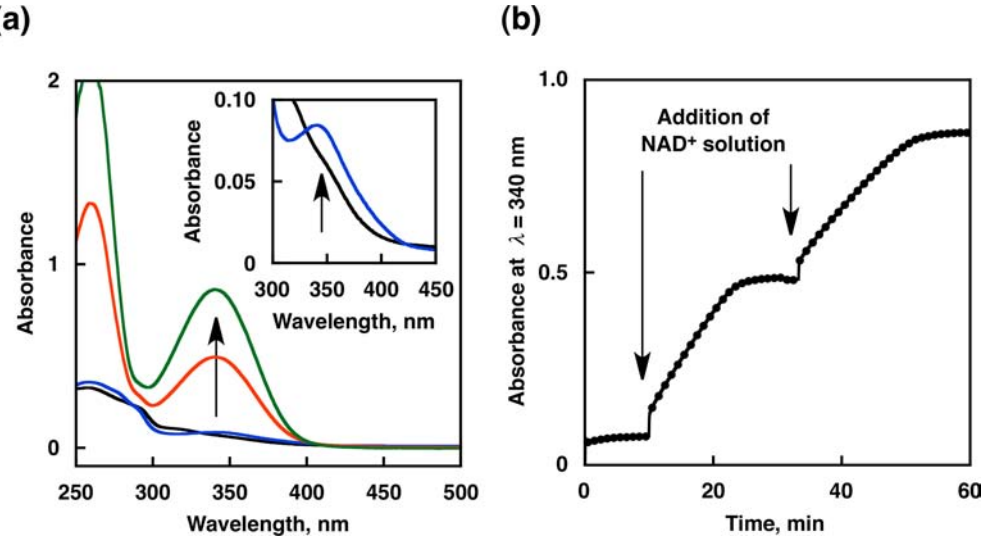

Figure 8. (a) UV−vis spectral change in the reaction of **2** and **3** ([**2**] +[**3**] = 15 μM) (black line) with ethanol (5.7 M) for 10 min (blue line), the UV−vis spectrum observed in the following reaction of NAD^+ (77 μM) with ethanol for 20 min (red line), and that observed in the reaction of NAD^+ with ethanol for 20 min (green line) after second addition of NAD^+ (77 μM) in the presence of **2** and **3** in a borate buffer at 298 K (pH 10.0). (b) Time course of absorbance at λ = 340 nm due to the reaction of **2** and **3** ([**2**] + [**3**] = 15 μM) with ethanol (5.7 M) and that due to the reaction of NAD^+ [initial concentration was 77 μM and the same concentration (77 μM) was added after the reaction] with ethanol catalyzed by **2** and **3** in a borate buffer at 298 K (pH 10.0).

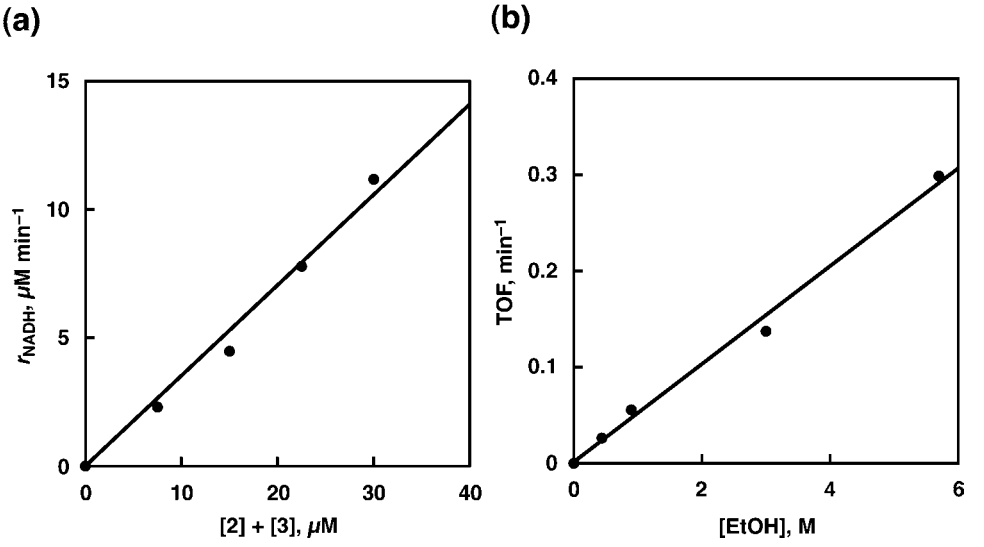

Figure 9. (a) Plot of formation rate of NADH versus concentration of **2** and **3** in the hydrogenation reaction of NAD^+ (77 μM) with ethanol (5.7 M) catalyzed by **2** and **3** in a deaerated borate buffer at 298 K and pH 10.0. (b) Plot of TOF for catalytic hydrogenation of NAD^+ versus concentration of ethanol in the hydrogenation reaction of NAD^+ (77 μM) with ethanol catalyzed by **2** and **3** ([**2**] + [**3**] = 15 μM) in a deaerated borate buffer at 298 K and pH 10.0.

Scheme 5

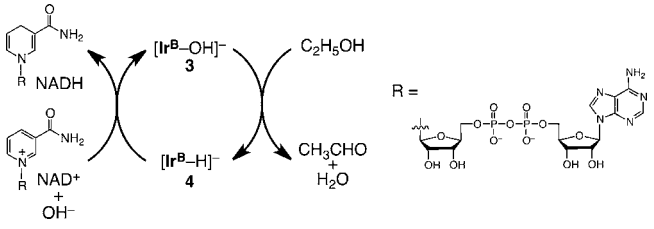

As previously reported, NAD^+ coordinated to **2** to afford the 1:1 complex. Thus, TOF of the catalytic hydrogenation of NAD^+ decreased with increasing concentration of NAD^+ (Figure 11a) due to the coordination of NAD^+ to **3** (Scheme 6), which makes it difficult to form the hydride complex.[24] In such a case, the formation rate of NADH (r_{NADH}, M h^{-1}) is given by eq 6, where $[\mathbf{3}]_i$ is the initial concentration of complex **3**. TOF_0 is the TOF value without the binding of NAD^+ to **3** and $TOF_0 = k_{obs}$. In eq 6, r_{NADH} is proportional to [**3**] as shown in Figure 9a. The binding constant K (M^{-1}) is expressed by eq 7. When [NAD^+] ≫ [**Ir**-NAD^+] and [NAD^+] ≫ [NADH], the TOF value is given by eq 8, which is converted to eq 9. As expected from eq 9, the plot of TOF^{-1} versus [NAD^+] (Figure 11b) shows a linear correlation. From the slope and intercept, the binding constant (K) of NAD^+ with **3** and TOF_0 were determined to be 2.7 × 10^3 M^{-1} and 21 h^{-1}, respectively. The TOF_0 value agrees well with the value (21 h^{-1}) independently determined from the absorption change

dx.doi.org/10.1021/ja302788c | J. Am. Chem. Soc. 2012, 134, 9417−9427

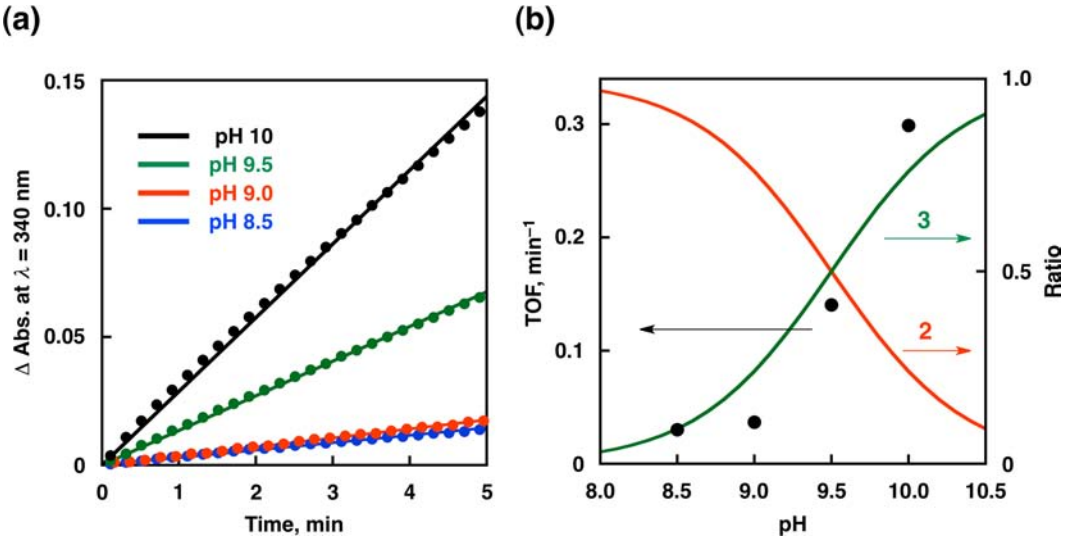

Figure 10. (a) Time course of absorbance at $\lambda = 340$ nm in the catalytic hydrogenation of NAD^+ (77 μM) with ethanol (5.7 M) to form NADH catalyzed by **2** and **3** ([**2**] + [**3**] = 15 μM) in a deaerated borate buffer at 298 K at various pH. Black, green, red, and blue lines represent time profiles at pH 10.0, 9.5, 9.0, and 8.5, respectively. (b) pH-Dependence of the formation rate (TOF) of NADH in the catalytic hydrogenation of NAD^+ (77 μM) with ethanol (5.7 M) catalyzed by **2** and **3** ([**2**] + [**3**] = 15 μM) in a deaerated borate buffer at 298 K (black dots). TOF values were determined based on the progress of the reaction for initial 5 min. Red and green solid lines show the amount ratios of complex **2** and complex **3**, respectively, to the total amount of the complexes.

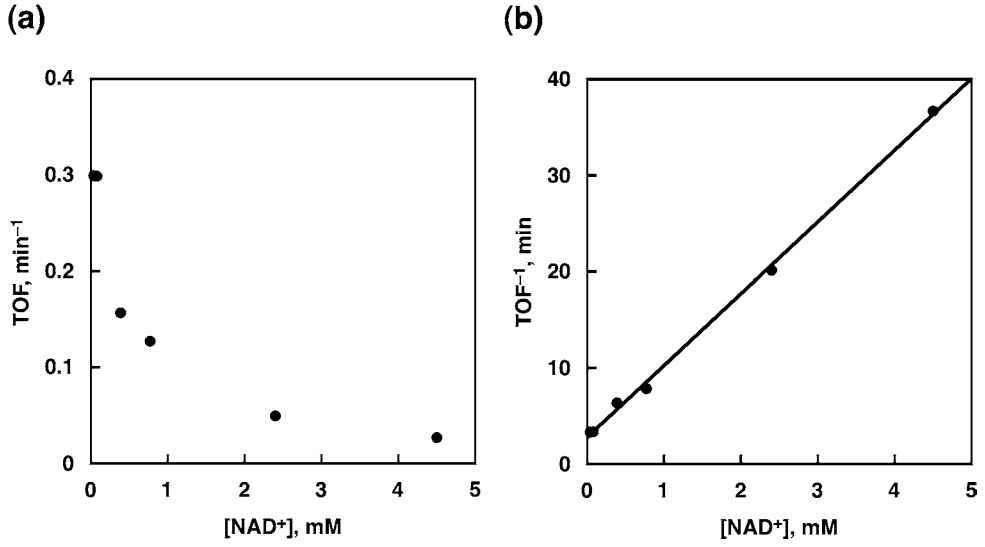

Figure 11. (a) Plot of TOF versus concentration of NAD^+ in the catalytic hydrogenation of NAD^+ with ethanol (4.1 M) to produce NADH under an atmospheric pressure in the presence of **2** and **3** ([**2**] + [**3**] = 15 μM) in a deaerated borate buffer (pH 10.0) at 298 K. TOF values were determined on the basis of the progress of the reaction for initial 5 min. (b) Plot of TOF^{-1} for the catalytic hydrogenation of NAD^+ with ethanol (5.7 M) in the presence of **2** and **3** ([**2**] + [**3**] = 15 μM) at 298 K (pH 10.0) versus concentration of NAD^+ according to eq 9.

Scheme 6

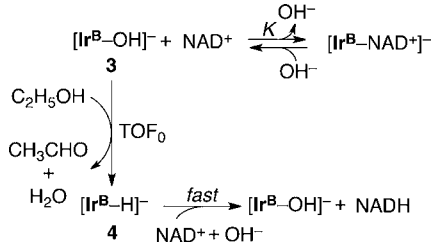

due to formation of **4** from **3** in the reaction of **3** with ethanol (vide supra).

$$r_{NADH} = TOF_0[\mathbf{3}] = TOF[\mathbf{3}]_i = TOF([\mathbf{3}] + [\mathbf{Ir^B}\text{-}NAD^+]) \quad (6)$$

$$K = [\mathbf{Ir^B}\text{-}NAD^+]/[NAD^+][\mathbf{3}] \quad (7)$$

$$TOF = TOF_0[\mathbf{3}]/([\mathbf{3}] + [\mathbf{Ir^B}\text{-}NAD^+]) = TOF_0(1 + [\mathbf{Ir^B}\text{-}NAD^+]/[\mathbf{3}]) = TOF_0/(1 + K[NAD^+]) \quad (8)$$

$$1/TOF = 1/TOF_0 + K[NAD^+]/TOF_0 \quad (9)$$

dx.doi.org/10.1021/ja302788c | J. Am. Chem. Soc. 2012, 134, 9417−9427

CONCLUSIONS

A mononuclear [C,N] cyclometalated half-sandwich iridium complex, $[Ir^{III}(Cp^*)(4\text{-}(1H\text{-pyrazol-1-yl-}\kappa N^2)\text{benzoic acid-}\kappa C^3)(H_2O)]_2SO_4$ $[\mathbf{1}]_2{\cdot}SO_4$, reacts with aliphatic alcohols to produce the corresponding hydride complex **4** at a high yield (98%) at pD 13.6 as confirmed by ESI mass spectrum, ^{1}H NMR, and UV−vis absorption spectra at room temperature. This is the first example of hydrogen production from aliphatic alcohols with **1** by changing pH at room temperature. The activation parameters of formation of the hydride complex were determined to be $\Delta H^{\ddagger}$ = 82 kJ mol^{-1} and $\Delta S^{\ddagger}$ = 1.5 J K^{-1} mol^{-1} from the Eyring plot. Photoirradiation of an aqueous solution of **4** resulted in formation of [C,C] cyclometalated Ir-hydride complex **5** (98%) at pD 13.6. Whereas **4** requires acidic conditions to produce H_2, the [C,C] cyclometalated Ir complex **5** acts as a catalyst for hydrogen evolution from 2-propanol and ethanol under basic conditions at ambient temperature. This is the first instance of hydrogen production from alcohols at ambient temperature. In the presence of ethanol at room temperature, NADH was catalytically regenerated from NAD^+ under basic conditions (pH 8.5−10.0) in the presence of complexes **2** and **3**. At pH 10.0, the TOF for the formation of NADH was up to 18 h^{-1}. At high NAD^+ concentrations, the hydrogenation reaction was retarded by the 1:1 complex formation between **3** and NAD^+. Thus, **2** and **3** act as efficient catalyst and functional mimics of alcohol dehydrogenase (ADH) for hydrogenation of NAD^+ to produce NADH in water.

ASSOCIATED CONTENT

Supporting Information

Figures S1−S11. This material is available free of charge via the Internet at http://pubs.acs.org.

AUTHOR INFORMATION

Corresponding Author

fukuzumi@chem.eng.osaka-u.ac.jp

Notes

The authors declare no competing financial interest.

ACKNOWLEDGMENTS

This work was partially supported by a Grant-in-Aid (No. 20108010 to S.F. and No. 21550061 to T.S.) and a Global COE program, "the Global Education and Research Centre for Bio-Environmental Chemistry" (to S.F.) from the MEXT, Japan, and NRF/MEST of Korea through WCU (R31-2008-000-10010-0) and GRL (2010-00353) Programs.

REFERENCES

(1) (a) *Hydrogen as a Future Energy Carrier*; Zuttel, A., Borgschulte, A., Schlapbach, L., Eds.; Wiley VCH: Weinheim, 2008. (b) Navarro, R. M.; M. A. Pena, M. A.; J. L. G. Fierro, J. L. G. *Chem. Rev.* **2007**, *107*, 3952. (c) Fukuzumi, S. *Eur. J. Inorg. Chem.* **2008**, 1351. (d) Fukuzumi, S.; Yamada, Y.; Suenobu, T.; Ohkubo, K.; Kotani, H. *Energy Environ. Sci.* **2011**, *4*, 2754. (e) Esswein, M. J.; Nocera, D. G. *Chem. Rev.* **2007**, *107*, 4022.

(2) (a) Fukuzumi, S.; Kobayashi, T.; Suenobu, T. *ChemSusChem* **2008**, *1*, 827. (b) Fukuzumi, S.; Kobayashi, T.; Suenobu, T. *J. Am. Chem. Soc.* **2010**, *132*, 1496. (c) Yamada, Y.; Yano, K.; Fukuzumi, S. *Energy Environ. Sci.* **2012**, *5*, 5356. (d) Yamada, Y.; Yano, K.; Xu, Q. A.; Fukuzumi, S. *J. Phys. Chem. C* **2010**, *114*, 16456.

(3) (a) Yamada, Y.; Miyahigashi, T.; Kotani, H.; Ohkubo, K.; Fukuzumi, S. *J. Am. Chem. Soc.* **2011**, *133*, 16136. (b) Fukuzumi, S.; Kotani, H.; Ono, T.; Ohkubo, K. *Phys. Chem. Chem. Phys.* **2007**, *9*, 1487. (c) Fukuzumi, S.; Kobayashi, T.; Suenobu, T. *Angew. Chem., Int. Ed.* **2011**, *50*, 728. (d) Kotani, H.; Hanazaki, R.; Ohkubo, K.; Yamada, Y.; Fukuzumi, S. *Chem.−Eur. J.* **2011**, *17*, 2777. (e) Kotani, H.; Ohkubo, K.; Takai, Y.; Fukuzumi, S. *J. Phys. Chem. B* **2006**, *110*, 24047.

(4) (a) Dempsey, J. L.; Winkler, J. R.; Gray, H. B. *J. Am. Chem. Soc.* **2010**, *132*, 16774. (b) Dempsey, J. L.; Winkler, J. R.; Gray, H. B. *J. Am. Chem. Soc.* **2010**, *132*, 1060.

(5) (a) McNamara, W. R.; Han, Z. J.; Alperin, P. J.; Brennessel, W. W.; Holland, P. L.; Eisenberg, R. *J. Am. Chem. Soc.* **2011**, *133*, 15368. (b) McCormick, T. M.; Calitree, B. D.; Orchard, A.; Kraut, N. D.; Bright, F. V.; Detty, M. R.; Eisenberg, R. *J. Am. Chem. Soc.* **2010**, *132*, 15480. (c) Lazarides, T.; McCormick, T.; Du, P. W.; Luo, G. G.; Lindley, B.; Eisenberg, R. *J. Am. Chem. Soc.* **2009**, *131*, 9192. (d) Du, P. W.; Knowles, K.; Eisenberg, R. *J. Am. Chem. Soc.* **2008**, *130*, 12576. (e) Du, P.; Schneider, J.; Fan, L.; Zhao, W.; Patel, U.; Castellano, F. N.; Eisenberg, R. *J. Am. Chem. Soc.* **2008**, *130*, 5056. (f) Zhang, J.; Du, P. W.; Schneider, J.; Jarosz, P.; Eisenberg, R. *J. Am. Chem. Soc.* **2007**, *129*, 7726. (g) Du, P. W.; Schneider, J.; Jarosz, P.; Eisenberg, R. *J. Am. Chem. Soc.* **2006**, *128*, 7726.

(6) (a) Lee, C. H.; Cook, T. R.; Nocera, D. G. *Inorg. Chem.* **2011**, *50*, 714. (b) Nocera, D. G. *Inorg. Chem.* **2009**, *48*, 10001.

(7) (a) Yamauchi, K.; Masaoka, S.; Sakai, K. *J. Am. Chem. Soc.* **2009**, *131*, 8404. (b) Ozawa, H.; Haga, M.; Sakai, K. *J. Am. Chem. Soc.* **2006**, *128*, 4926. (c) Ozawa, H.; Sakai, K. *Chem. Commun.* **2011**, *47*, 2227.

(8) (a) Stubbert, B. D.; Peters, J. C.; Gray, H. B. *J. Am. Chem. Soc.* **2011**, *133*, 18070. (b) Lee, C. H.; Dogutan, D. K.; Nocera, D. G. *J. Am. Chem. Soc.* **2011**, *133*, 8775.

(9) (a) Huang, L.; Liu, Q.; Chen, R.; Hsu, A. *Appl. Catal., A* **2011**, *393*, 302. (b) Haryanto, A.; Fernando, S.; Murali, N.; Adhikari, S. *Energy Fuels* **2005**, *19*, 2098. (c) Huber, G. W.; Shabaker, J. W.; Dumesic, J. A. *Science* **2003**, *300*, 2075. (d) Haryanto, A.; Fernando, S.; Murali, N.; Adhikari, S. *Energy Fuels* **2005**, *19*, 2098.

(10) (a) Johnson, T. C.; Morris, D. J.; Wills, M. *Chem. Soc. Rev.* **2010**, *39*, 81. (b) Friedrich, A.; Schneider, S. *ChemCatChem* **2009**, *1*, 72.

(11) (a) Román-Leshkov, Y.; Barrett, C. J.; Liu, Z. Y.; Dumesic, J. A. *Nature* **2007**, *447*, 982. (b) Chheda, J. N.; Huber, G. W.; Dumesic, J. A. *Angew. Chem., Int. Ed.* **2007**, *46*, 7164.

(12) Cortright, R. D.; Davda, R. R.; Dumesic, J. A. *Nature* **2002**, *418*, 964.

(13) Sieffert, N.; Bühl, M. *J. Am. Chem. Soc.* **2010**, *132*, 8056.

(14) Johansson, A. J.; Zuidema, E.; Bolm, C. *Chem.−Eur. J.* **2010**, *16*, 13487.

(15) (a) Junge, H.; Loges, B.; Beller, M. *Chem. Commun.* **2007**, 522. (b) Yang, L.-C.; Ishida, T.; Yamakawa, T.; Shinoda, S. *J. Mol. Catal.* **1996**, *108*, 87. (c) Morton, D.; Cole-Hamilton, D. J.; Utuk, D.; Paneque-Sosa, M.; Lopez-Poveda, M. *J. Chem. Soc., Dalton Trans.* **1989**, 489. (d) A. Dobson, A.; Robinson, St. D. *Inorg. Chem.* **1977**, *16*, 137.

(16) *Handbook of Chemistry and Physics*, 89th ed.; Lide, D. R., Ed.; CRC Press: Boca Raton, FL, 2008−2009.

(17) (a) Wiberg, K. B.; Crocker, L. S.; Morgan, K. M. *J. Am. Chem. Soc.* **1991**, *113*, 3447. (b) Pink, M.; Eisenstein, O. *J. Chem. Educ.* **2002**, *79*, 1269. (c) Huang, L.; Liua, Q.; Chena, R.; Hsu, A. T. *Adv. Catal., A* **2011**, *393*, 302.

(18) Nielsen, M.; Kammer, A.; Cozzula, D.; Junge, H.; Gladiali, S.; Beller, M. *Angew. Chem., Int. Ed.* **2011**, *50*, 9593.

(19) Kawahara, R.; Fujita, K.; Yamaguchi, R. *J. Am. Chem. Soc.* **2012**, *134*, 3643.

(20) Catalytic hydrogen production in alcohols as a solvent has been reported;[18] however, catalytic hydrogen production from water-soluble alcohols, e.g., ethanol, 2-propanol, in water has yet to be achieved.[19]

(21) Pirez, C.; Capron, M.; Jobic, H.; Dumeignil, F.; Jalowiecki-Duhamel, L. *Angew. Chem., Int. Ed.* **2011**, *50*, 10193.

(22) Ni, M.; Leung, D. Y. C.; Leung, M. K. H. *Int. J. Hydrogen Energy* **2007**, *32*, 3238.

(23) Sarkar, N.; Ghosh, S. K.; Bannerjee, S.; Aikat, K. *Renewable Energy* **2012**, *37*, 19.

(24) Maenaka, Y.; Suenobu, T.; Fukuzumi, S. *J. Am. Chem. Soc.* **2012**, *134*, 367.

(25) Maenaka, Y.; Suenobu, T.; Fukuzumi, S. *Energy Environ. Sci.* **2012**, DOI: 10.1039/c2ee03315a.
(26) (a) Magnuson, A.; Anderlund, M.; Johansson, O.; Lindblad, P.; Lomoth, R.; Polivka, T.; Ott, S.; Stensjö, K.; Styring, S.; Sundström, V.; Hammarström, L. *Acc. Chem. Res.* **2009**, *42*, 1899. (b) Ghirardi, M. L.; Dubini, A.; Yu, J.; Maness, P. C. *Chem. Soc. Rev.* **2009**, *38*, 52. (c) Malki, S.; Saimmaime, I.; Luca, D. G.; Rousset, M.; Dermoun, Z.; Belaich., J. P. *J. Bacteriol.* **1995**, *177*, 2628. (d) Soboh, B.; Linder, D.; Hedderich., R. *Microbiology* **2004**, *150*, 2451. (e) Schut, G. J.; Adams, W. W. *J. Bateriol.* **2009**, *191*, 4451. (f) Liebgott, P.-P.; De Lacey, A. L.; Burlat, B.; Cournac, L.; Richaud, P.; Brugna, M.; Fernandez, V. M.; Guigliarelli, B.; Rousset, M.; Léger, C.; Dementin, S. *J. Am. Chem. Soc.* **2011**, *133*, 986.
(27) (a) Ruppert, R.; Herrmann, S.; Steckhan, E. *J. Chem. Soc., Chem. Commun.* **1988**, 1150. (b) Westerhausen, D.; Herrmann, S.; Hummel, W.; Steckhan, E. *Angew. Chem., Int. Ed.* **1992**, *31*, 1529.
(28) (a) Fish, R. H.; Lo, H. C.; Buriez, O.; Kerr, J. B. *Angew. Chem., Int. Ed.* **1999**, *38*, 1429. (b) Lo, H. C.; Leiva, C.; Buriez, O.; Kerr, J. B.; Olmstead, M. M.; Fish, R. H. *Inorg. Chem.* **2001**, *40*, 6705. (c) Lo, H. C.; Fish, R. H. *Angew. Chem., Int. Ed.* **2002**, *41*, 478. (d) Lutz, J.; Hollmann, F.; Ho, T. V.; Schnyder, A.; Fish, R. H.; Schmid, A. *J. Organomet. Chem.* **2004**, *689*, 4783.
(29) Hollmann, F.; Witholt, B.; Schmid, A. *J. Mol. Catal. B: Enzym.* **2002**, *19*, 167.
(30) Wagenknecht, P. S.; Penney, J. M.; Hembre, R. T. *Organometallics* **2003**, *22*, 1180.
(31) Salmain, M.; Haquette, P.; Talbi, B.; Barilleau, L.; Madern, N.; Fosse, C. *Org. Biomol. Chem.* **2011**, *9*, 5720.
(32) Bhoware, S. S.; Kim, K. Y.; Kim, J. A.; Wu, Q.; Kim, J. *J. Phys. Chem. C* **2011**, *115*, 2553.
(33) Wienkamp, R.; Steckhan, E. *Angew. Chem., Int. Ed.* **1983**, *22*, 497.
(34) (a) Lee, S. H.; Nam, D. H.; Kim, J. H.; Baeg, J. O.; Park, C. B. *ChemBioChem* **2009**, *10*, 1621. (b) Park, C. B.; Lee, S. H.; Subramanian, E.; Kale, B. B.; Lee, S. M.; Baeg, J. O. *Chem. Commun.* **2008**, 5423. (c) Lee, S. H.; Ryu, J.; Nam, D. H.; Park, C. B. *Chem. Commun.* **2011**, *47*, 4643.
(35) (a) Chen, D.; Yang, D.; Wang, Q.; Jiang, Z. Y. *Ind. Eng. Chem. Res.* **2006**, *45*, 4110. (b) Jiang, Z. Y.; Lu, C. Q.; Wu, H. *Ind. Eng. Chem. Res.* **2005**, *44*, 4165.
(36) Makinen, M. W.; Maret, W.; Yim, M. B. *Proc. Natl. Acad. Sci. U.S.A.* **1983**, *80*, 2584.
(37) Kimura, E.; Shionoya, M.; Hoshino, A.; Ikeda, T.; Yamada, Y. *J. Am. Chem. Soc.* **1992**, *114*, 10134.
(38) Kolle, U.; Franzl, H. *Monatsh. Chem.* **2000**, *131*, 1321.
(39) (a) Parkin, G. *Chem. Rev.* **2004**, *104*, 699. (b) Dolega, A. *Coord. Chem. Rev.* **2010**, *254*, 916.
(40) Glasoe, P. K.; Long, F. A. *J. Phys. Chem.* **1960**, *64*, 188.
(41) Klei, S. R.; Golden, J. T.; Burger, P.; Bergman, R. G. *J. Mol. Catal. A: Chem.* **2002**, *189*, 79.
(42) Noziere, B.; Chabert, P. *Int. J. Chem. Kinet.* **2010**, *42*, 676.
(43) Pocker, Y.; Meany, J. E. *J. Phys. Chem.* **1967**, *71*, 3113.
(44) Kurz, J. L.; Coburn, J. I. *J. Am. Chem. Soc.* **1967**, *89*, 3528.
(45) Blum, O.; Milstein, D. *J. Am. Chem. Soc.* **1995**, *117*, 4582.
(46) Ichimura, K.; Kobayashi, T.; King, K. A.; Watts, R. J. *J. Phys. Chem.* **1987**, *91*, 6104.
(47) Tang, K. C.; Liu, K. L.; Chen, I. C. *Chem. Phys. Lett.* **2004**, *386*, 437.
(48) Hrobarik, P.; Hrobarikova, V.; Meier, F.; Repisky, M.; Komorovsky, S.; Kaupp, M. *J. Phys. Chem. A* **2011**, *115*, 5654.
(49) Johnston, C. C.; Gardner, J. L.; Suelter, C. H.; Metzler, D. E. *Biochemistry* **1963**, *2*, 689.
(50) Hilvers, A. G.; van Dam, K. *Biochim. Biophy. Acta* **1964**, *81*, 391.
(51) Alberty, R. A. *Arch. Biochem. Biophys.* **1998**, *353*, 116.